J Mater Sci (2010) 45:5101–5108
DOI 10.1007/s10853-010-4478-4

ICAM 2009

Spatial organization of peptide nanotubes for electrochemical devices

T. C. Cipriano · P. M. Takahashi · D. de Lima · V. X. Oliveira Jr. · J. A. Souza · H. Martinho · W. A. Alves

Received: 30 November 2009 / Accepted: 5 April 2010 / Published online: 22 April 2010

Abstract A novel biosensor for hydrogen peroxide was developed by combining the known properties of microperoxidase-11 (MP11) as an oxidation catalyst, and the interesting properties of diphenylalanine peptide nanotubes (PNTs) as a supporting matrix to allow a good bioelectrochemical interface. In this case, the synthesized MP11/PNTs were immobilized onto the ITO electrode surface via layer-by-layer (LBL) deposition, using poly(allylamine hydrochloride) (PAH) as positively charged polyelectrolyte layers. The PNTs provide a favorable microenvironment for MP11 to perform direct electron transfer to the electrode surface. The resulting electrodes showed a pair of well-defined redox peaks with formal potential at about −343 mV (versus SCE) in phosphate buffer solution (pH 7). The experimental results also demonstrated that the resulting biosensor exhibited good electrocatalytic activity to the reduction of H_2O_2 with a sensitivity of 9.43 μA cm^{-2} $mmol^{-1}$ L, and a detection limit of 6 μmol L^{-1} at the signal-to-noise ratio of 3. Moreover, we also observed that the peptides self-assembly can be influenced upon changing the pH of the solution. Alkaline solution appears to favor the packing of diphenylalanine nanotubes being closer than acidic or neutral conditions. The study proved that the combination of PNTs with MP11 is able to open new opportunities for the design of enzymatic biosensors with potential applications in practice.

T. C. Cipriano · P. M. Takahashi · D. de Lima · V. X. Oliveira Jr. · J. A. Souza · H. Martinho · W. A. Alves (✉)
Centro de Ciências Naturais e Humanas, Universidade Federal do ABC, Santo André, SP, Brazil
e-mail: wendel.alves@ufabc.edu.br

T. C. Cipriano · P. M. Takahashi · D. de Lima · W. A. Alves
Instituto Nacional de Ciência e Tecnologia de Bioanalítica, P.O. Box 6154, Campinas, SP 13083-970, Brazil

Introduction

In natural biological systems, macromolecules exert exceptional control over inorganic nucleation, phase stabilization, assembly, and pattern formation [1]. Biological systems assemble nanoscale-building blocks into complex and functionally sophisticated structures with high perfection, controlled size, and compositional uniformity [2]. These materials are typically soft and consist of a surprisingly simple collection of molecular building blocks (i.e., lipids, peptides, and nucleic acids) arranged in complex architectures [3]. The controlled self-assembly of biomolecular structures, preferably from the simplest building blocks possible, is therefore of great interest for future nanotechnological applications [4]. Results of recent studies have demonstrated that peptide nanostructures have great potential to serve as structural and functional elements in various applications, such as drug delivery agents, scaffolds for tissue engineering, biosensing devices, and also as a template for the nanofabrication of metallic and other inorganic materials [5].

Besides their easy design and synthesis, short peptides are both excellent model systems for the study of biological self-assembly and ideal building blocks for the production of a wide range of biological materials [6]. Aromatic dipeptides consisting of two successively connected phenylalanine units have been regarded as an important building block for nanofabrication [7]. Recently, Gazit and co-workers have studied the mechanism of amyloid fibril formation and thermal and chemical stability of PNTs

[8, 9]. Particularly, diphenylalanine peptide nanotubes (PNTs) represent the core recognition reason of Alzheimer's β-amyloid polypeptide [10]. The significant thermal and chemical stability of this material has demonstrated the potential use of diphenylalanine peptide in future applications, such as micro-fabrication processes [11] and functional nanodevices [12]. It has been suggested that besides intermolecular hydrogen bonding, the rigid aromatic side chains may be responsible for stability and mechanical strength of PNTs. Such aromatic chains provide directionality for formation through specific π–π interactions as well. This notion has recently gained much experimental and theoretical support [13]. Moreover, Kim and co-workers have also determined the morphological diversity of the self-assembly of diphenylalanine units in various polar solvents [14]. Nanotubes were fabricated in water and nanoribbons were prepared in methanol and ethanol. In nonpolar solvents, such as dichloromethane, both nanoribbons and nanowires were obtained. The morphological evolution of one-dimensional structures is assumed to originate from the subtle balance between hydrogen bonding and hydrophobic interaction.

Numerous ways for anchoring electrochemically active compounds onto electrode surfaces have been investigated aiming the shortening of the distance between the redox sites involved in the electron-transfer reaction [15]. Especially with peroxidases, direct electron transfer has been demonstrated, and horseradish peroxidase has been used successfully as a biocatalytic compound for the construction of biosensors and biofuel cells [16]. Microperoxidase-11 (MP11) is a small redox protein obtained by proteolytic digestion of horse heart cytocrome *c*. It consists of an iron containing porphyrinic system connected to an α-helical undecapeptide via two thioether bonds [17]. The sixth coordination site of the heme group is vacant and accessible to a number of exogenous ligands [18]. Electrochemical studies have shown that MP11 can exhibit enzymatic activity similar to peroxidase enzymes [19]. As a consequence of its small size, a high surface concentration can be obtained even when a monolayer is formed. A major drawback for the application of microperoxidases is their limited stability under turnover conditions.

The aim of this work is to study the intercalation of MP11 with diphenylalanine PNTs. This interaction was studied by scanning electron microscopy (SEM), X-ray powder diffractogram, FTIR, diffuse reflectance, and electrochemical measurements in order to analyze the binding conformations and electronic properties between protoporphyrin IX and PNTs. Electrochemical studies have shown direct electron transfer between MP11 immobilized self-assembled PNTs and the electrode via layer-by-layer (LBL) deposition.

Experiment

Materials

The MP11 was purchased from Sigma-Aldrich Corp., and used as received without further purification. Acetonitrile (ACN), acetic acid (CH_3COOH), trifluoroacetic acid (TFA), sodium hydroxide, dichloromethane, methylformamide, methanol, poly(allylamine hydrochloride) (PAH), thietylamine, buffers, and all other reagents were purchased from Sigma-Aldrich. Phosphate buffer solutions (ca. 0.1 mol L^{-1}) of different pHs were prepared from stock solutions containing NaH_2PO_4 and Na_2HPO_4. All solutions were prepared using ultra-pure water (Millipore, resistivity 18 MΩ cm^{-1}). Amino acid derivative was purchased from Novabiochem. All other chemicals were of reagent grade and used without further purification. The LBL films were assembled onto ITO-coated glass (indium–tin oxide, one-side coated on glass by Delta Technologies).

Instruments

SEM experiments were recorded on a JEOL FEG-SEM (JSM 6330F) or a JEOL LV-SEM (JSM 5900LV) microscope of the LME/LNLS (Laboratory of Electron Microscopy of the Brazilian Synchrotron Light Laboratory, Campinas, Brazil). X-ray diffraction (XRD) patterns of powdered samples were recorded on a Rigaku diffractometer Minifelx model using Cu Kα radiation. Optical absorbance spectra and diffuse reflectance spectra were recorded in a Varian Cary-50 Bio spectrophotometer using the diffuse reflectance accessory. FTIR spectra of solid samples were recorded on a Varian spectrometer, model 660-IR, with a reflectance accessory. The purity of products was determined on high-performance liquid chromatography (HPLC, model 600, Waters). The LC/ESI-MS data were obtained on a Micromass instrument, model ZMD coupled on a Waters Alliance model 2690 system. The materials were centrifuged using a centrifuge MPW, model 350. Cyclic voltammetry (CV) and chronoamperometry (CA) experiments were performed with an Autolab PGSTAT30 (EcoChemie) electrochemical system. All potentials are referred to a saturated calomel electrode (SCE) while a platinum foil was employed as the auxiliary electrode. Before experiments, the buffer solution was bubbled with pure nitrogen for a thoroughly anaerobic condition, and the gas stream was maintained over the solution during the measurements.

Peptide synthesis and purification

The diphenylalanine was synthesized using common protocol for manual solid-phase methodology and *t*-Boc strategy [20, 21]. The N^{α}-terminal temporary protecting

group was removed with 50% TFA in DCM in the presence of 2% anisole for 20 min. Couplings were carried out using 2.5 excess of DIC in DCM–DMF (1:1, v/v) and were monitored by Kaiser ninhydrin test [22]. The dry protected peptidyl-resin was exposed to anhydrous HF in the presence of 10% anisole at 0 °C for 1.5 h. Excess HF and scavenger were eliminated under high vacuum. The crude peptides were precipitated with anhydrous diethylether, separated by filtration and extracted from the resin with 50% acetic acid in H_2O and lyophilized. The crude product was purified by preparative HPLC (Waters C_{18} DeltaPak 21 × 250 mm; eluted with A 0.1% TFA/H_2O, B 1% TFA/60% ACN/H_2O; gradient from 25 to 55% B over 90 min; flow: 10 mL min^{-1}; detection: UV at 220 nm). Selected fractions containing the purified peptide were pooled [23], and subsequently characterized by liquid chromatography/electrospray ionization mass spectrometry (LC/ESI-MS).

Peptide nanostructure preparation (PNTs)

Fresh stock solutions were prepared by dissolving the lyophilized form of the peptides in 1,1,1,3,3,3-hexafluoro-2-propanol at a concentration of 100 mg mL^{-1}. The peptide stock solutions were diluted to 5 mg mL^{-1} in ultra-pure water. For the formation of PNTs of differential pH (3, 7, and 12) using the peptide stock solutions and then diluted down with water contended CH_3COOH or NaOH (1 mol L^{-1}) at a final concentration of 5 mg mL^{-1}. To avoid any preaggregation, fresh stock solutions were prepared for each experiment.

Immobilization of microperoxidase-11 at diphenylalanine peptide nanotubes (MP11/PNTs)

The nanotubes solution at concentration of 5 mg mL^{-1} from the fresh stock solutions was centrifuged for 15 min in a MPW centrifuge at 12000 × rpm. The supernatant was removed and the precipitate was washed with ultra-pure water and centrifuged for 15 min. To this precipitate were added of the solutions of different concentrations of MP11 (7.44×10^{-2} g L^{-1}, 14.88×10^{-2} g L^{-1}) and they were then aged under stirring for 12 h. The MP11/PNTs were centrifuged and washed with ultra-pure water three times to remove excess MP11.

Preparation of the modified ITO electrode by LBL techniques

LBL films were prepared by alternately immersing ITO substrate three times for 20 min in PAH solution (0.5 g L^{-1}/pH 7), and for 10 min in MP11/PNTs suspension. The modified substrate was washed in ultra-pure water and dried with nitrogen.

Results and discussions

SEM analysis

The self-assembly of diphenylalanine compounds was investigated under acidic, neutral, and basic conditions by varying the pH of the medium used. The nanometric structures formed by the diphenylalanine compound (L-Phe···L-Phe) correspond to well-ordered, fibrillar, and elongated assemblies as seen by SEM techniques (Fig. 1). The nanotubes were obtained from a solution of L-Phe···L-Phe in 1,1,1,3,3,3-hexafluoro-2-propanol, which were further diluted in H_2O containing the pH of the solution previously adjusted to 3, 7, and 12 by adding a few drops of freshly prepared CH_3COOH or NaOH (1 mol L^{-1}) solution. The average fiber diameter appeared to be comparable to other nanotubular structures described for diphenylalanine [6, 14, 24], which is a broad distribution with average ∼120 nm. The fibrils are very long (several micrometers) and usually appear to be laterally associated. A change from pH 3–12 alters not only charge distributions but also intermolecular hydrogen bonds among peptide monomers that determine the formation of such assembled structures. The morphology of the fundamental tubular unit remained unchanged over the range of pH used. However, in acid and basic solutions

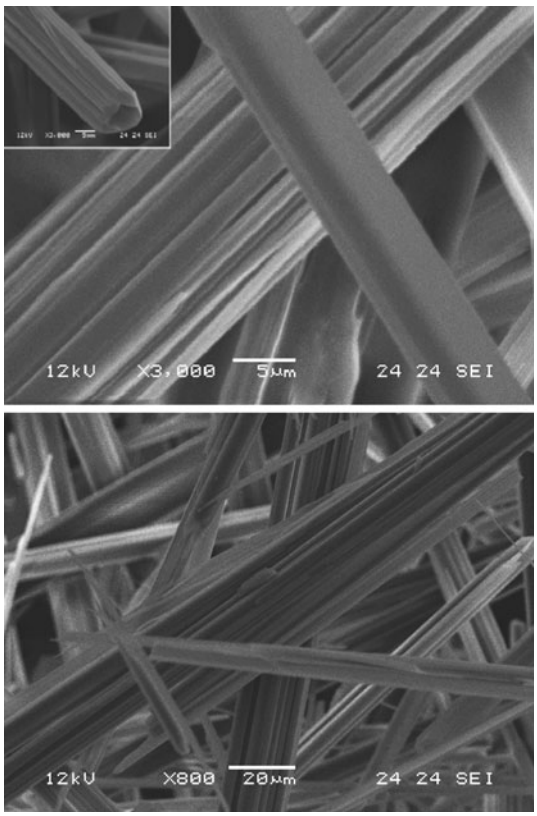

Fig. 1 SEM images showing PNT packing prepared in pH 12 solution

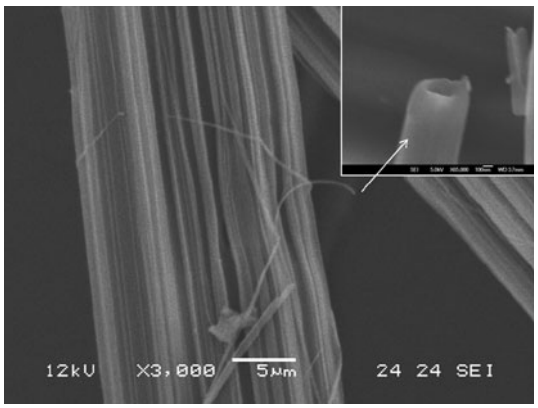

Fig. 2 SEM images showing stability of the diphenylalanine PNTs prepared in pH 7 solution containing microperoxidase-11 intercalated among the different hexagonal layers of such nanotubes

we observed more lateral association of the PNTs, probably due to variation of dipolar interactions and specific intermolecular hydrogen bonding. Particularly in pH 12, we observed a more efficient packing among PNT structures than in the configuration of pH 3 and 7. In this case, the degree of carboxylic acid and amino group protonation can be used to control the final assembled structures, since the structures are determined by the strengths of the amide–amide and COO^-/NH_3^+ group interactions [25].

After that, we studied the immobilization of MP11 in PNTs. The SEM of the iron protoporphyrin IX intercalated in diphenylalanine nanotubes is shown in Fig. 2. A hollow structure of the template nanotube was preserved after the metalloprotoporphyrin was immobilized on the nanotube surfaces, as shown in insert of Fig. 2. However, significant differences in the aggregated structure for (MP11/PNTs) prepared in pH 7 solutions have been obtained, despite what had been anticipated. The carboxylic acid residue from protoporphyrin IX and peptide chain can be involved in the link between MP11 and the amide groups of the tubule template. Evidence of the existence of intermolecular hydrogen bonds among them may be obtained by infrared spectroscopy and XRD, which will be discussed later. In this case, we observed that there was an efficient packing of diphenylalanine nanotubes at pH 7 when there was MP11 intercalated on their surfaces. Furthermore, the same assembled structure obtained for diphenylalanine nanotubes prepared in solution of pH 12 was observed for (MP11/PNTs), as shown in Fig. 2. It seems that proteins are capable of interacting with the tubule free amide sites via hydrogen bonds and then produce more aggregation among PNT structures.

XRD

Figure 3 shows powder XRD patterns of the diphenylalanine nanotubes prepared in solutions of pH 7 and 12 and

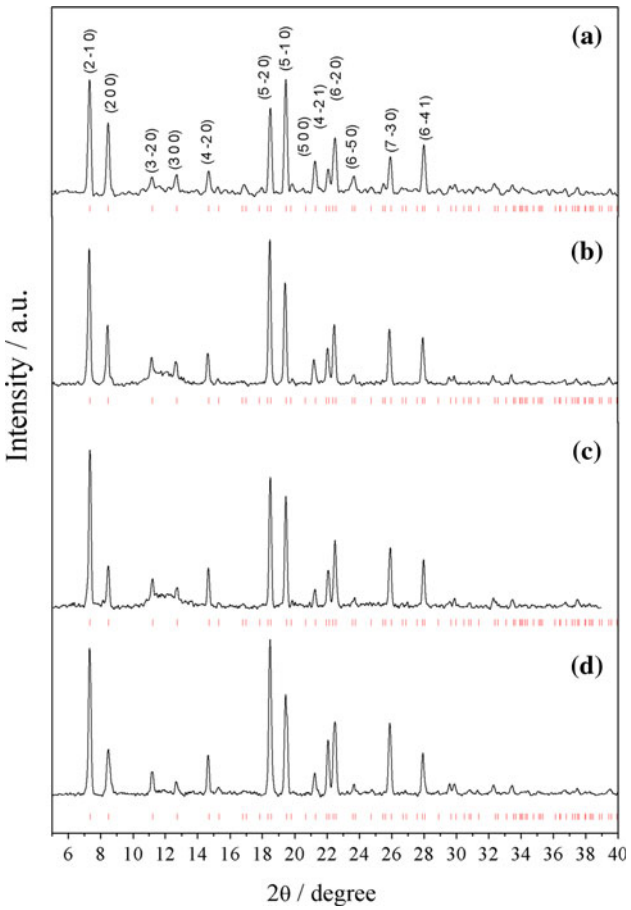

Fig. 3 X-ray diffraction patterns of samples prepared in solution of pH 7 (**a**) and 12 (**b**) and with different MP11 concentration in PNT structures: 7.44×10^{-2} g L^{-1} (**c**) and 14.9×10^{-2} g L^{-1} (**d**). Tick marks under the experimental profiles indicate the positions of the allowed Bragg reflections for the hexagonal ($P6_1$) space group symmetry. The respective crystallographic planes are also shown for the most intense peaks

with different MP11 concentration. All the observed plane reflections have been indexed as belonging to the hexagonal space group $P6_1$. This is in agreement with a PNT structure symmetry which was recently proposed by Gorbitz [13]. In addition, a careful inspection of the XRD profiles reveals the absence of extra reflections belonging to any additional crystal phase.

We have systematically observed that not only the samples prepared in different pH solutions but also with different MP11 concentrations change the distance between crystallographic planes, bringing about different cell parameters. For instance, the refined cell parameters of the samples were found to be: PNTs (pH 7) $a = b =$ 24.1824 Å and $c = 5.3944$ Å; PNTs (pH 12) $a = b =$ 24.1373 Å and $c = 5.3988$ Å; MP11/PNTs (pH 7, [MP11] $= 7.44 \times 10^{-2}$ g L^{-1}) $a = b = 24.1795$ Å and $c = 5.4036$ Å; MP11/PNTs (pH 7, [MP11] $= 14.9 \times 10^{-2}$ g L^{-1}) $a = b = 24.0975$ Å and $c = 5.41455$ Å.

As observed in X-ray diffractogram, there has been an accentuated decrease in signal intensity in the variation of pH and also in the presence of MP11 in pH 7, probably due to the decrease of the aperture sizes of the nanotubes. Moreover, we have observed not only a decrease in the cell parameters *a* and *b* but also an increase in *c* parameter, which is probably due to the intercalation of MP11 between the different hexagonal layers of the nanotubes [13, 26].

Spectroscopy characterization

In order to get information regarding the secondary structures of the self-assembled nanostructures of L-Phe···L-Phe in solution of different pHs, FTIR spectra were used. Diphenylalanine nanotubes not only differ from each other by length and width but also in their secondary structure conformation due to pH variations of the solution. A curve fitting procedure can be applied to estimate quantitatively the area of each component, representing a type of secondary structure. The amide I was deconvoluted with Lorentzian line shape functions through an interactive curve fitting procedure. After that, the structural components were quantified by the integrated areas of the respective peaks. The amide I bands at 1686 and 1695 cm^{-1} are assigned to β-turn and β-sheet conformation, respectively [27–29]. The relationship between these peaks for PNTs prepared in pH 7 solution indicated that the β-turn structure corresponds to 63 percent of the β-sheet peak area at 1695 cm^{-1}. However, in pH 12 the spectrum for L-Phe···L-Phe peptide indicated a decrease of the β-turn conformation in relation to pH 7, corresponding now to 38 percent of the β-sheet peak area, and also presenting a predominant anti-parallel β-sheet structure with maximum absorption peaks at 1623, 1634, 1640, 1674, and 1690 cm^{-1}. This result suggests that the stronger amide–amide hydrogen bonds in pure solid β-sheet conformation, obtained in alkaline solution, seem to pack diphenylalanine nanotubes closer than acidic or neutral conditions, corroborating with results from SEM discussed before.

The free amide sites on the tubules can also form hydrogen bonds with molecules containing amide or carboxylic acid groups [30, 31]. Thus, we applied FTIR to study the interaction of MP11 and the template PNTs for future sensor applications. In this case, the carboxylic acid ion group from MP11 can be adsorbed on the tubule surface as shown in Fig. 2, and also as previously demonstrated by XRD. Most of the peaks in the neat protoporphyrin IX spectrum appear in the MP11/PNT spectrum [32, 33]. The most dominating signals in the mid infrared range can be clearly attributed to the carbonyl stretching mode of the protonated heme propionates at 590 cm^{-1} [32]. The ν(C=O) mode from protoporphyrin IX appears at 1698 and 1716 cm^{-1} in the MP11/PNT spectrum [32]. This peak is shifted in comparison with the carbonyl stretch in solid state, probably due to hydrogen bonds between the carbonyl group of protoporphyrin IX and the amide group of PNTs. A similar attachment mechanism was also utilized to produce metalloporphyrin nanotubes [33]. Absorbance spectrum of the amide I band at 1683 cm^{-1} indicated a dominant β-sheet conformation, similar to diphenylalanine nanotubes prepared in solution of pH 12 (Fig. 4).

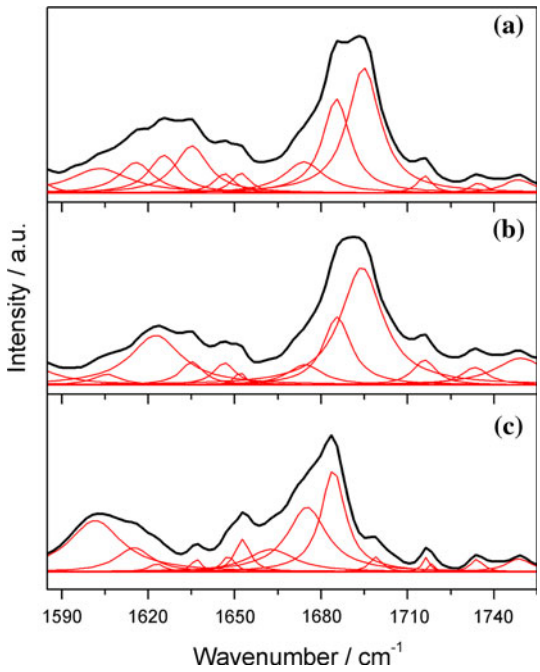

Fig. 4 FTIR spectra of PNTs prepared in pH 7 (**a**) and pH 12 (**b**) and MP11/PNTs hybrid structures (**c**). The individual deconvoluted bands with Lorentzian line shape functions are shown as *solid curves*

To qualitatively investigate the biological activity of heme proteins immobilized on PNT structures, the change of the Soret band at 410 nm before and after immobilization was also observed. The position of a Soret absorption band of Fe(III) heme can provide information about possible denaturing of heme proteins [34, 35]. As depicted in Fig. 5, the position and shape of adsorption bands at 410 and 520 nm for MP11/PNT was almost the same as those for free MP11 in solid state, suggesting that the heme protein entrapped in the PNT structures has similar conformation to the native structure. The *Q* band at ~520 nm was similar to that of oxidized MP11 and there was no evidence of a charge transfer band during the diphenylalanine PNTs interaction.

Electrochemical characteristics of the modified electrode

The direct electron transfer of MP11 immobilized in the diphenylalanine PNTs structure was investigated by CV.

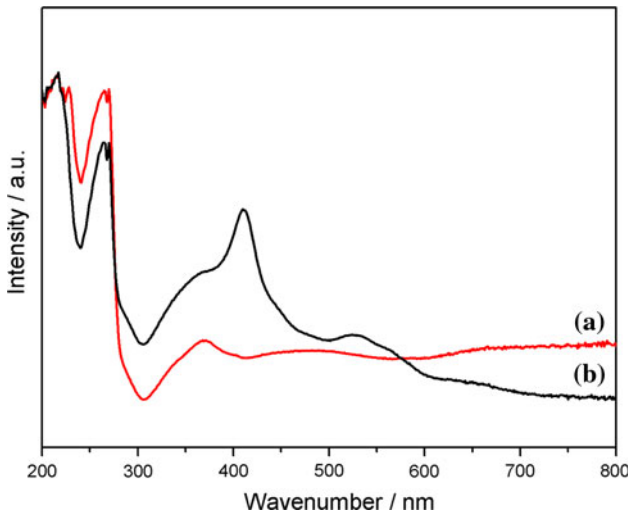

Fig. 5 Diffuse reflectance spectra of PNTs (*a*) and MP11/PNTs (*b*)

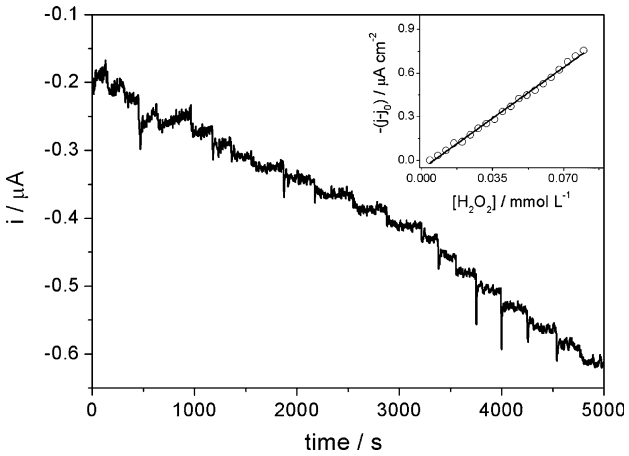

Fig. 7 Response of the modified electrode $(MP11/PNTs/PAH)_{n=4}$/ITO to H_2O_2, added in portions of 4 μmol L^{-1}. The electrode was operated at −0.3 V (versus SCE), in 0.1 mol L^{-1} PBS (pH 7)

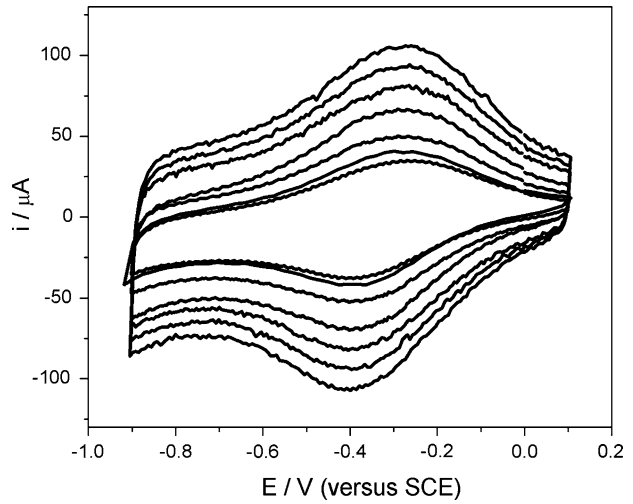

Fig. 6 Cyclic voltammograms of $(MP11/PNTs/PAH)_{n=4}$/ITO in PBS (0.1 mol L^{-1}) at scan rates from 0.5 to 3.5 V s^{-1}

Figure 6 shows the cyclic voltammograms for four layers of $(MP11/PNTs/PAH)_{n=4}$ attached to an ITO electrode at different scan rates in 0.1 mol L^{-1} phosphate buffer solution (pH 7). A pair of redox peaks with the formal potential of −343 mV (versus SCE) was observed for the hybrid films, a value which is in good agreement with the measured formal potential of MP11 immobilized on nanocomposite containing single-walled carbon nanotubes and gold nanoparticles [36]. The electrochemical reaction can be assigned to heme Fe^{III}/Fe^{II} redox couples of the heme protein [37]. This suggests that the MP11 immobilized on the PNT structure surface has successfully kept its bioelectroactivity.

To examine the sensitivity of the prepared $(MP11/PNTs/PAH)_{n=4}$/ITO electrode, we investigated the amperometric response of H_2O_2 in the stirring pH 7 PBS solution. The applied potential was set at −300 mV versus SCE, where the amperometric response reaches the maximum value. Figure 7 shows the typical current–time curves for the modified electrode with a successive addition of H_2O_2. The cathodic reduction currents at about −300 mV increased linearly with the increasing H_2O_2 concentration, as shown in inset of Fig. 7. Upon the addition of H_2O_2, the $(MP11/PNTs/PAH)_{n=4}$/ITO electrode reaches its maximum steady-state response within 5 s, indicating a fast diffusion process and a high activity of the MP11 in this system. The sensitivity has been estimated to be 9.43 μA cm^{-2} $mmol^{-1}$ L, and the detection limit was 6 μmol L^{-1} at the signal-to-noise ratio of 3. These values are expressive when compared with other procedures that involve immobilization of MP11 onto electrode surface that have already been reported in literature (see Table 1). These values demonstrate that the PNTs can provide a bridge of electron transfer between protein and electrode. The large value obtained to detection limit can be related to the isolating characteristic of this material, due to wide semiconductor-like band gaps when compared to other semiconductor-like organic molecules.

Further studies also showed that this biosensor is very stable. When it was stored at 4 °C for 2 weeks and used for measurements intermittently, the sensor retained more than 85% of its initial response to the reduction of 0.1 mmol L^{-1} H_2O_2. This long-term stability can be attributed to the strong interactions between the PNTs and MP11. However, when the concentration of H_2O_2 is higher than 3 mmol L^{-1}, the immobilized MP11 is denatured and irreversibly transformed to its oxidized, inactive form. The good electrochemical response, stability, and reproducibility of $(MP11/PNTs/PAH)_{n=4}$/ITO electrode demonstrates the high

Table 1 Comparison of developed H_2O_2 biosensor with other systems containing microperoxidases, HRP or cytochrome *c* immobilized on the surface of the modified electrodes

H_2O_2 biosensor enzyme electrode	Sensitivity ($\mu A\ cm^{-2}\ mmol^{-1}\ L$)	Detection limit ($\mu mol\ L^{-1}$)	Reference
$(MP11/PNTs/PAH)_{n=4}$/ITO	9.43	6	This work
MP11/MWCNTs/PtE	–	0.7	[38]
MP11/Nafion/MWCNTs–$BPPF_6$/GCE	–	0.0038	[39]
MP11/GCE	3.6	–	[40]
MP11/HCPE	0.12	–	[40]
MP11/GNPs/MWNTs/GCE	628	3	[37]
HRP/silver-NPs/CYS/Au	0.70	0.78	[41]
MP11/lipid membrane/GCE	–	0.8	[42]
MP8/PPY/GCE	0.89	0.0037	[43]
MP11/MWNTs/Pt microelectrode	0.0578	0.7	[44]
Cyt c/Cys/GNPs/Chits/MWNTs/GC	92.21	0.9	[45]

activity of the MP11. This can be attributed to the diphenylalanine PNTs, which supply a biological environment on the surface of the ITO electrode to maintain the active configuration of the enzymes. This also demonstrates that PNTs are an ideal choice to immobilize enzymes for applications in oxidase-based biosensors.

Conclusions

We have shown that the packing of the diphenylalanine nanotubes is favored in alkaline solution and such behavior also appeared on their secondary structures as demonstrated by electron microscopy and FTIR techniques. Moreover, we have observed the intercalation of MP11 between the different hexagonal layers of the nanotubes through XRD and electronic spectroscopy. The LBL methods were found to be efficient for immobilization of the hybrid nanomaterial MP11/PNTs onto the electrode surface. The obtained results revealed that direct electron transfer between redox proteins and the underlying electrode can be easily performed at the $(MP11/PNTs/PAH)_{n=4}$ hybrid film electrode, and the PNT structures have shown good biocompatibility and high surface activity to attach MP11. This modified ITO electrode displays good catalytic reduction effect for H_2O_2 reduction, with good sensitivity ($9.43\ \mu A\ cm^{-2}\ mmol^{-1}\ L$) and detection limit ($6\ \mu mol\ L^{-1}$). PNTs can be expanded to immobilize other proteins and improve their electrocatalytic capability.

Acknowledgements Financial support by the Brazilian agencies *Fundação de Amparo à Pesquisa do Estado de São Paulo* (FAPESP, Grant No. 08/51074-6, 08/53576-9, 05/53241-9 and 08/55549-9) is gratefully acknowledged. This work was also supported by INCT in Bioanalytics (FAPESP, Grant No. 08/57805-2 and CNPq, Grant No. 573672/2008-3). We are also thankful to LME–LNLS (Project SEM–LV 9004 and SEM–FEG 8511).

References

1. Zhang S (2003) Nat Biotechnol 21:1171
2. Sarikaya M (1999) Proc Natl Acad Sci USA 96:14183
3. Seeman NC, Belcher AM (2002) PNAS 99:6451
4. Kohli P, Martin CR (2005) Curr Pharm Biotechnol 6:35
5. Scanlon S, Aggeli A (2008) Nano Today 3:22
6. Gao X, Matsui H (2005) Adv Mater 17:2037
7. Reches M, Gazit E (2006) Phys Biol 3:S10
8. Reches M, Gazit E (2003) Science 300:625
9. Adler-Abramovich L, Reches M, Sedman VL, Allen S, Tendler SJB, Gazit E (2006) Langmuir 22:1313
10. de Groot NS, Parella T, Aviles FX, Vendrell J, Ventura S (2007) Biophys J 92:1732
11. Sopher NB, Abrams ZR, Reches M, Gazit E, Hanein Y (2007) J Micromech Microeng 17:2360
12. Yemini M, Reches M, Gazit E, Rishpon J (2005) Anal Chem 77:5155
13. Gorbitz CH (2006) Chem Commun 2332
14. Han TH, Park JS, Oh JK, Kim SO (2008) J Nanosci Nanotechnol 8:5547
15. Alves WA, Fiorito PA, Froyer G, Haber FE, Vellutini L, Torresi RM, Cordoba de Torresi SI (2008) J Nanosci Nanotechnol 8:3570
16. Katz E, Sheeney-Haj-Ichia L (2006) Angew Chem Int Ed 43:3292
17. Nicolis S, Casella L, Roncone R, Dallacosta C, Monzani E (2007) C R Chimie 10:1
18. Dallacosta C, Alves WA, Ferreira AMDC, Monzani E, Casella L (2007) J Chem Soc Dalton Trans 21:2197
19. Lotzbeyer T, Schuhmann W, Katz E, Falter J, Schmidt H-L (1994) J Electroanal Chem 377:291
20. Merrifield RB (1963) J Am Chem Soc 85:2149
21. Matsueda GR, Stewart JM (1981) Peptides 2:45
22. Kaiser E, Bossinger CD, Colescott RL, Olsen DB (1980) Anal Chim Acta 118:149
23. Oliveira VX, Fazio MA, Santos EL, Pesquero JB, Miranda A (2008) J Pept Sci 14:617
24. Yan X, Cui Y, He Q, Wang K, Li J (2008) Chem Mater 20:1522
25. Matsui H, Gologan B (2000) J Phys Chem B 104:3383
26. Gorbitz CH (2001) Chem Eur J 7:5153
27. Castelletto V, Hamley IW, Harris PJF, Olsson U, Spencer N (2009) J Phys Chem B 113:9978
28. Surewicz WK, Mantsch HH, Chapman D (1993) Biochemistry 32:389

29. Nagai Y, Nakanishi T, Okamoto H, Takeda K, Furukawa Y, Usui K, Mihara H (2005) Jpn J Appl Phys 44:7654
30. Douberly GE Jr, Pan S, Walters D, Matsui H (2001) J Phys Chem B 105:7612
31. Matsui H, Pan S, Douberly GE Jr (2001) J Phys Chem B 105:1683
32. Dorr S, Schade U, Hellwig P (2008) Vib Spectrosc 47:59
33. Matsui H, MacCuspie R (2001) Nano Lett 1:671
34. George P, Hanania G (1952) Biochem J 52:517
35. Donoghue DO, Magner E (2007) Electrochim Acta 53:1134
36. Jiang H-J, Zhao Y, Yang H, Akins DL (2009) Mater Chem Phys 114:879
37. Liu Y, Wang M, Zhao F, Guo Z, Chen H, Dong S (2005) J Electroanal Chem 581:1
38. Munteanu FD, Lindgren A, Emnéus J, Gorton L, Ruzgas T, Csoregi E, Ciuru A, van Huystee RB, Gazaryan IG, Lagrimini LM (1998) Anal Chem 70:2596
39. Wan J, Bi J, Du P, Zhang S (2009) Anal Biochem 386:256
40. Razumas V, Kazlauskaite J, Vidziunaite R (1996) Bioelectrochem Bioenerg 39:139
41. Ren C, Song Y, Li Z, Zhu G (2005) Anal Bioanal Chem 381:1179
42. Huang W, Jia J, Zhang Z, Han X, Tang J, Wang J, Dong S, Wang E (2003) Biosens Bioelectron 18:1225
43. Korri-Youssoufi H, Desbenoit N, Ricoux R, Mahy J-P, Lecomte S (2008) Mater Sci Eng C 28:855
44. Wang M, Zhao F, Liu Y, Dong S (2005) Biosens Bioelectron 21:159
45. Xiang C, Zou Y, Sun L-X, Xu F (2007) Talanta 74:206